Medium corrections in the formation of light charged particles in heavy ion reactions

C. Kuhrts,[1] M. Beyer,[1,*] P. Danielewicz,[2] and G. Röpke[1]
[1]*FB Physik, Universität Rostock, Universitätsplatz 3, D-18051 Rostock, Germany*
[2]*NSCL, Michigan State University, East Lansing, Michigan 48824*
(Received 13 September 2000; published 12 February 2001)

Within a microscopic statistical description of heavy ion collisions, we investigate the effect of the medium on the formation of light clusters. The dominant medium effects are self-energy corrections and Pauli blocking that produce the Mott effect for composite particles and enhanced reaction rates in the collision integrals. Microscopic description of composites in the medium follows the Dyson equation approach combined with the cluster mean-field expansion. The resulting effective few-body problem is solved within a properly modified Alt-Grassberger-Sandhas formalism. The results are incorporated in a Boltzmann-Uehling-Uhlenbeck simulation for heavy ion collisions. The number and spectra of light charged particles emerging from a heavy ion collision change in a significant manner in effect of the medium modification of production and absorption processes.

DOI: 10.1103/PhysRevC.63.034605 PACS number(s): 25.70.−z, 24.10.Cn, 21.45.+v, 21.65.+f

I. INTRODUCTION

The description of the dynamics of an interacting many-body system is particularly difficult when the quasiparticle approach reaches its limits. That may be the case when the residual interaction is strong enough to build up correlations. An example of such a system with correlations is nuclear matter in heavy-ion collisions. In collisions, the nuclear matter is first compressed and excited and then decompressed. At another extreme of the macroscopic scale, the nuclear matter is formed during a supernova collapse and becomes the material of which a neutron star is made.

Here, we address the simplest case of the formation of correlations in a nonequilibrium situation: light-cluster production in low density nuclear matter. The production can be described microscopically following the set of generalized semiclassical Boltzmann equations. In the past, the coupled set was solved numerically for nucleon f_N, deuteron f_d, triton f_t, and helium-3 f_h Wigner functions within the Boltzmann-Uehling-Uhlenbeck (BUU) approach [1,2]. The formation and disintegration of clusters generally takes place in reactions involving different particles. The rates for respective processes are utilized in the Boltzmann collision integrals.

Rates for collisions, whether involving clusters or not, are central ingredients of all modern microscopic approaches to heavy reactions such as the Boltzmann-Uehling-Uhlenbeck (BUU) approach [1–4] or the quantum molecular dynamics (QMD) [5,6]. For the status of those approaches see Ref. [7].

The formation and disintegration of deuterons are the simplest types of processes involving clusters discussed above. Notably, with the exception of electromagnetic production and breakup ($np \rightleftharpoons \gamma d$), these processes involve the minimum of three elementary particles ($NNN \rightleftharpoons Nd$) and, correspondingly, require the solution of a three-body problem in the medium in their description. Complication brought in by the medium is evident even in the kinematics, as the medium brings in a preferred frame different from the center of mass of the three bodies.

In general, the collision rates are affected by the surrounding medium. The common procedure is to ignore the medium dependence and to utilize free-space *experimental cross sections*. That procedure in many cases was very successful. To calculate the rates, including the *self-energy shift* and the proper *Pauli blocking*, and to study the influence of the medium on different observables, a generalized Alt-Grassberger-Sandhas (AGS) equation [8] has been derived [9–15]. The effective few-body problem in matter arises within the Green function method [16] when following the cluster mean-field expansion [17] or the Dyson equation approach [18]. Besides the medium-dependent cross sections, the Mott effect [19,20] plays an important role in nuclear matter. Both effects are studied in this paper in the context of a realistic simulation of a heavy ion reaction. As an example we choose the reaction studied in a recent experiment by the INDRA Collaboration, namely ^{129}Xe+^{119}Sn at 50 MeV/nucleon [21].

The BUU approach will be explained in the following section. The needed three-body reaction input from the AGS-type equations will be discussed in Sec. III. Details of the derivation of these equations within the Green function approach may be, e.g., found in Ref. [16]. In Sec. IV we shall present numerical results and in the last section we shall summarize the paper and give conclusions.

II. NUCLEAR REACTIONS

Within the microscopic statistical approach, the reacting system is described in terms of the Wigner distributions f_X for light particles, thus for nucleon f_N, deuteron f_d, triton f_t, and helion f_h. Within the cluster mean-field

*Corresponding author: FB Physik, Universität Rostock, Universitätsplatz 3, D-18051 Rostock, Germany. Phone: [+49] 381/498-1674, Fax: -1673. Electronic address: michael.beyer@physik.uni-rostock.de

approximation, these distributions follow the set of coupled semiclassical Boltzmann equations [1],

$$\partial_t f_X + \{\mathcal{U}_X, f_X\} = \mathcal{K}_X^{\rm gain}\{f_N, f_d, f_t, \dots\}(1 \pm f_X) - \mathcal{K}_X^{\rm loss}\{f_N, f_d, f_t, \dots\} f_X, \quad X = N, d, t, \dots . \tag{1}$$

In the above, $\mathcal{U}_X$ is a mean-field potential and $\{\cdot,\cdot\}$ denotes the Poisson bracket. The upper sign on the right-hand side (rhs) is for the Bose and the lower for the Fermi-type fragments. Conversion between different species is accounted for in the collision integrals $\mathcal{K}\{f_N, f_d, f_t, \dots\}$. For example, the deuteron gain rate $\mathcal{K}_d^{\rm gain}(P,t)$ is

$$\mathcal{K}_d^{\rm gain}(P,t) = \int d^3k \int d^3k_1\, d^3k_2 |\langle kP|U|k_1k_2\rangle|^2_{dd\to dd} f_d(k_1,t) f_d(k_2,t) \overline{f}_d(k,t) + \int d^3k \int d^3k_1\, d^3k_2 |\langle kP|U|k_1k_2\rangle| \Big|^2_{Nd\to Nd} f_N(k_1,t) f_d(k_2,t) \overline{f}_N(k,t) + \int d^3k \int d^3k_1\, d^3k_2\, d^3k_3 |\langle kP|U_0|k_1k_2k_3\rangle|^2_{pnN\to dN} f_N(k_1,t) f_N(k_2,t) f_N(k_3,t) \overline{f}_N(k,t) + \cdots . \tag{2}$$

Here we use the abbreviations $\overline{f}_N = (1 - f_N)$ and $\overline{f}_d = (1 + f_d)$ and did not write overall energy-momentum conserving δ functions. The ellipsis on the rhs of Eq. (2) denotes further possible contributions from four and more body collisions (e.g., $tp \rightleftharpoons dd$, $hp \rightleftharpoons dd$) or electromagnetic ($np \rightleftharpoons \gamma d$). The loss rate $\mathcal{K}_d^{\rm loss}(P,t)$ is given by

$$\mathcal{K}_d^{\rm loss}(P,t) = \int d^3k \int d^3k_1\, d^3k_2\, d^3k_3 |\langle k_1k_2k_3|U_0|kP\rangle|^2_{dN\to pnN} \times \overline{f}_N(k_1,t) \overline{f}_N(k_2,t) \overline{f}_N(k_3,t) f_N(k,t) + \cdots . \tag{3}$$

The quantity U_0 appearing in Eqs. (2) and (3) is the in-medium breakup transition operator for the $Nd \to NNN$ reaction and it is calculated using the AGS equation, as discussed in the next section. For three nucleons in isolation, U_0 determines free-space breakup cross section $\sigma_{\rm bu}^0$ via the equation [8,22]

$$\sigma_{\rm bu}^0(E) = \frac{1}{|v_d - v_N|} \frac{1}{3!} \int d^3k_1\, d^3k_2\, d^3k_3 |\langle kP|U_0|k_1k_2k_3\rangle|^2 \times 2\pi\delta(E' - E)(2\pi)^3 \delta^{(3)}(k_1 + k_2 + k_3), \tag{4}$$

where $|v_d - v_N|$ denotes the relative velocity of the incoming nucleon and deuteron. This equation along with detailed balance is used to replace the squared transition matrix elements by the breakup cross section [1]. The cross sections can be extracted from data with theory aiding in interpolating and extrapolating. This type of procedure is widely used and has a good chance of being successful in the low density regime. However, this procedure may not be sufficient for heavy ion collisions particularly in the lower energy regime. The elementary cross section that enters into the Boltzmann equation depends on the medium, e.g., through blocking of intermediate states in scattering or through self-energy for intermediate states. This has been demonstrated for three-nucleon processes in Refs. [9,11].

III. FINITE TEMPERATURE FEW-BODY EQUATIONS

The effective few-body problem in matter emerges within the Green function method [16] when following the cluster expansion [17] or related Dyson-equation approach [18]. In the cluster-mean field expansion, a self-consistent system of equations can be derived describing an A particle cluster moving in a mean field produced by the equilibrium mixture of clusters with different particle number. The self-consistent determination of the composition of the medium is a very challenging task that is not solved until now. We adhere to an approximation where the correlations in the medium outside the considered cluster are neglected so that the embedding nuclear matter is described by the equilibrium distribution of nucleon quasiparticles.

The formalism to describe three-body correlations in nuclear matter has been discussed in detail elsewhere [9–15]. Here, we merely repeat some of the basic results for convenience.

Let the Hamiltonian of the system be given by

$$H = \sum_1 \frac{k_1^2}{2m} a_1^\dagger a_1 + \frac{1}{2} \sum_{121'2'} V_2(12,1'2')\ a_1^\dagger a_2^\dagger a_{2'} a_{1'}, \tag{5}$$

where a_1 denotes the Heisenberg annihilation operator of the particle with quantum numbers indexed by 1, including spin s_1 and momentum k_1. The free resolvent G_0 for an A particle cluster is given in the Matsubara-Fourier representation by

$$G_0(z) = (z - H_0)^{-1}\ N \equiv R_0(z)\ N. \tag{6}$$

In the above, G_0, H_0, and N are all operators in the space of A particles. For simplicity, an index A indicating that fact has been dropped, but may get instituted when needed. In Eq.

(6), z denotes the Matsubara frequencies $z_\lambda=\pi\lambda/(-i\beta)+\mu$ with $\lambda=0,\pm2,\pm4,\ldots$ for bosons and $\lambda=\pm1,\pm3,\ldots$ for fermions; μ is the chemical potential and $\beta=1/k_BT$ the inverse temperature. The effective in-medium Hamiltonian H_0 for the quasiparticles in the mean field is given by

$$H_0=\sum_{i=1}^{n}\frac{k_i^2}{2m}+\Sigma_i\equiv\sum_{i=1}^{n}\varepsilon_i, \tag{7}$$

where the energy shift Σ_1 is

$$\Sigma_1=\sum_2 V_2(12,\widetilde{12})f_2, \tag{8}$$

with the Fermi function f_1

$$f_1\equiv f(\varepsilon_1)=\frac{1}{e^{(\varepsilon_1-\mu)/k_BT}+1}. \tag{9}$$

The tilde in $\widetilde{12}$ indicates antisymmetrization. The factor N in Eq. (6) is associated with particle statistics and it is given by

$$N=\overline{f}_1\overline{f}_2\cdots\overline{f}_A\pm f_1f_2\cdots f_A, \tag{10}$$

where $\overline{f}=1-f$. The upper sign in N is for an odd number of constituent fermions and the lower sign is for an even number of fermions or bosons. Note that the commutation holds: $NR_0=R_0N$.

The full resolvent G in the Matsubara-Fourier representation may be written as

$$G(z)=(z-H_0-V)^{-1}N\equiv R(z)N, \tag{11}$$

where the potential V is a sum over two-body interactions within all possible pairs α in the cluster, i.e.,

$$V=\sum_\alpha V_\alpha=\sum_\alpha N_2^\alpha V_2^\alpha, \tag{12}$$

where V_2^α denotes the two-body potential in Eq. (5). Note that, in consequence of Eq. (12), the effective potential is non-Hermitian, $V^\dagger\neq V$, and also $R(z)N\neq NR(z)$. This leads to the necessity of introducing the right and left eigenvectors as, e.g., done in the context of the four-body problem in Ref. [15]. For a pair $\alpha=(12)$ of an A particle cluster, the effective potential of Eq. (12) is

$$\langle 12|N_2^{(12)}V_2^{(12)}|1'2'\rangle=(\overline{f}_1\overline{f}_2-f_1f_2)V_2(12,1'2'). \tag{13}$$

A useful operator is the channel resolvent $G_\alpha(z)$ within an A particle cluster, where only effective pair interaction in channel α is considered. This operator may be represented as

$$G_\alpha(z)=(z-H_0-V_\alpha)^{-1}N=(z-H_0-N_2^\alpha V_2^\alpha)^{-1}N \equiv R_\alpha(z)N. \tag{14}$$

Using inverses to the operators R defined in Eqs. (6), (11), and (14), it is possible to derive formally the resolvent equations. For the sake of similarity with the isolated case, the A particle channel t matrix T_α is defined by

$$R_\alpha(z)=R_0(z)+R_0(z)T_\alpha(z)R_0(z). \tag{15}$$

Upon introducing $T_\alpha(z)=N_2^\alpha T_2^\alpha(z)$, Eq. (15) yields to the well-known Feynman-Galitzki equation [16]

$$T_2^\alpha(z)=V_2^\alpha+V_2^\alpha R_0(z)N_2^\alpha T_2^\alpha(z). \tag{16}$$

We remark that equations of a similar form were derived by different authors in the past [23,24].

Note that the above equations are also valid for the two-particle subsystem embedded in a larger cluster (three, four, or more particles). As for the isolated equations, the effects of the remaining particles appear only in the Matsubara frequencies z (energies) of the considered particles within the cluster. No additional statistical factors related to the larger cluster arise. One should note that the statistical effects generally arise in the resolvent G_0 and not in the potential V_2. However, it is possible to rewrite the respective equations introducing an effective potential, as shown in Eq. (16), and instead using unchanged resolvents. Following the more intuitive picture of the blocking in the propagation of the particles, described by the resolvents, we directly find in Eq. (16) the proper expression for the t matrix which enters the Boltzmann collision integrals (see, e.g., Ref. [25]).

Derivation of the three-body in-medium equation is relatively straightforward and was given in Refs. [11–14]. The AGS operator $U_{\beta\alpha}(z)$ [8] for the three-particle system is defined within the equation

$$R(z)=\delta_{\beta\alpha}R_\alpha(z)+R_\beta(z)U_{\beta\alpha}(z)R_\alpha(z), \tag{17}$$

and it satisfies the following AGS-type equation:

$$U_{\beta\alpha}(z)=\overline{\delta}_{\beta\alpha}R_0(z)^{-1}+\sum_\gamma \overline{\delta}_{\beta\gamma}N_2^\gamma T_2^\gamma(z)R_0(z)U_{\gamma\alpha}(z). \tag{18}$$

This equation includes consistently the medium effects, statistical and self-energy shifts in the same way as the Feynman-Galitzki equation for the two-particle correlations. We use above the notation $\overline{\delta}_{\alpha\beta}=1-\delta_{\alpha\beta}$. The AGS-type equation yields the three-body transition operator U for a three-particle cluster as well the transition operator for a three-particle cluster embedded in a still larger cluster. In the latter case, the effect of the other particles in the cluster appears only in the Matsubara frequency (energy) z. The transition operator is defined in Eq. (17) in such a manner that no additional factors N accompany U when U is further employed. This in turn guarantees that the cluster equations are valid also if they are part of a larger cluster. The two-body subsystem t matrix entering in Eq. (18) is the same as the one given in Eq. (16). In that way it is possible to use all results of the few-body algebra recurrently, in particular those based on the cluster decomposition property.

The in-medium bound state equation for an A particle cluster follows from the homogeneous Lippmann-Schwinger-type equation

$$|\psi_B\rangle = R_0(E_B)V|\psi_B\rangle = R_0(E_B)\sum_\gamma N_2^\gamma V_2^\gamma|\psi_B\rangle, \quad (19)$$

where the sum is over all unique pairs in the cluster. As shown in Ref. [13], it is convenient to introduce the form factors for the three-body bound state:

$$|F_\beta\rangle = \sum_{\gamma=1}^{3} \overline{\delta}_{\beta\gamma} N_2^\gamma V_2^\gamma|\psi_{B_3}\rangle. \quad (20)$$

With these, one derives the homogeneous in-medium AGS-type equation

$$|F_\alpha\rangle = \sum_{\beta=1}^{3} \overline{\delta}_{\alpha\beta} N_2^\beta T_2^\beta R_0(B_3)|F_\beta\rangle. \quad (21)$$

Since the Green functions are evaluated in an independent particle basis, the one-, two-, and three-particle Green functions are decoupled in hierarchy. To solve the in-medium problem up to three-particle clusters, the one-, two-, and three-particle problems are solved consistently. The procedure generates the single particle self-energy shift, given by Eq. (8), the two-body input including statistical factors in Eq. (16), and, finally, the three-body scattering state.

When solving the equations, technical reasons force us to adopt some reasonable approximations valid at smaller effective densities. Thus, the nucleon self-energy is calculated via Eq. (8), but in the three-body equations we employ the effective-mass approximation, i.e., we use

$$\varepsilon_1 = \frac{k_1^2}{2m} + \Sigma^{\rm HF}(k_1) \simeq \frac{k_1^2}{2m^*} + \Sigma^{\rm HF}(P_{\rm c.m.}/3). \quad (22)$$

For the sake of simplicity and the speed of the calculation, we moreover utilize angle-averaged Fermi-function factors $\overline{N}_2$,

$$\overline{N}_2(p,q,P_{\rm c.m.}) = \frac{1}{(4\pi)^2}\int d\cos\theta_q\, d\cos\theta_p\, d\phi_q\, d\phi_p \times N_2(\mathbf{p},\mathbf{q},\mathbf{P}_{\rm c.m.}), \quad (23)$$

where $\mathbf{p}$ and $\mathbf{q}$ are the standard Jacobi coordinates [22] and the angles are relative to $\mathbf{P}_{\rm c.m.}$.

Rank-one Yamaguchi potentials [26] were employed in the calculations of the deuteron breakup cross section in the coupled $^3S_1 - ^3D_1$ and the $^1S_0$ channels which should suffice at low energies. Through the dependence of the Fermi functions on the center of mass momentum, the integral equation for the three-body system exhibits a dependence on the net momentum in the medium frame, in sharp contrast to the free-space case.

IV. RESULTS

The coupled set of Boltzmann transport equations [1,2], for the Wigner distribution functions of nucleons f_N, deuterons f_d, tritons f_t, and helions f_h, is solved for the collisions of heavy ions. For the clusters, treated in the quasiparticle approximation, it is essential to consider the Mott effect [1,19,20]. Without considering this effect the description of data fails badly.

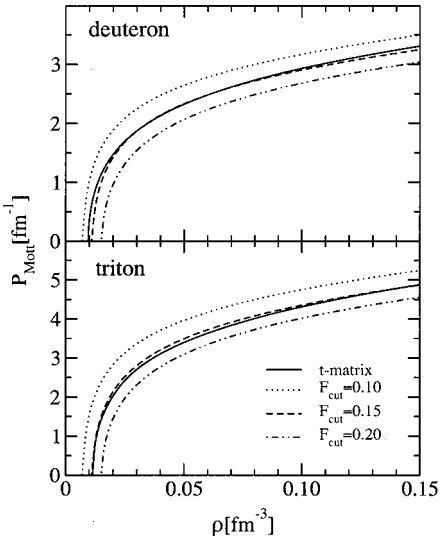

FIG. 1. Deuteron and triton Mott momenta $P_{\rm Mott}$ shown as a function of density ρ at fixed temperature of $T=10$ MeV. The solid line represents results of the *t* matrix approach. The dashed, dotted, and dashed-dotted lines represent the deuteron Mott momenta from the parametrization given in Eq. (24) for three different cutoff values $F_{\rm cut}$.

The Mott effect occurs when a bound state wave function requires too many momenta components in the regime already occupied by momenta of other particles (Pauli blocked). In Ref. [1] a geometrical model was introduced in order to account for the Mott effect in a numerical solution of the transport equations (1). Specifically, in the model the formation of a quasiparticle cluster is allowed only if the overlap of the respective isolated bound state wave function ϕ and the Fermi sphere given in Eq. (9) is lower then a specific cutoff value $F_{\rm cut}$. For the deuteron, the formation is then allowed if [1]

$$\int d^3q\ f\left(\mathbf{q}+\frac{\mathbf{P}_{\rm c.m.}}{2}\right)\ |\phi(\mathbf{q})|^2 \leqslant F_{\rm cut}, \quad (24)$$

where $\mathbf{P}_{\rm c.m.}$ denotes the net momentum of the bound state in the medium frame and $\mathbf{q}$ denotes the relative momentum of the nucleons in the deuteron. The cutoff $F_{\rm cut}$ needs to be specified and it enters as a parameter the collision simulation. For the clusters in the Boltzmann equation set, we use the calculated deuteron and triton Mott momenta [13,27] to restrict the choices for the parameter $F_{\rm cut}$. Note, however, that the procedure is not completely stringent since the methods of calculating the Mott momenta, following the geometrical picture and the *t* matrix approach, are different. The differently calculated Mott momenta are shown in Fig. 1 for the temperature $T=10$ MeV. No bound states are possible for the region below a respective curves in Fig. 1. As seen in Fig. 1, the parametrization given in Eq. (24) with a cutoff value of $F_{\rm cut}=0.15$ fits reasonably the microscopic calcula-

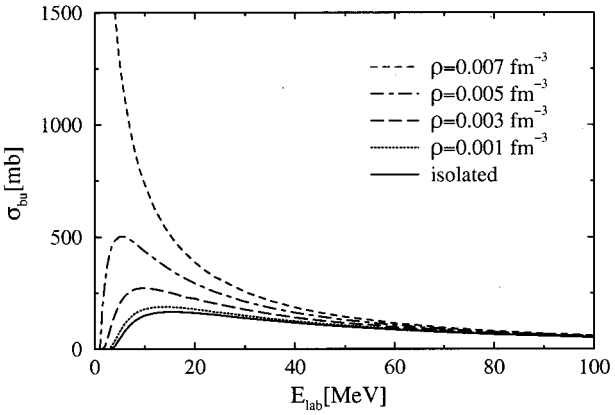

FIG. 2. Neutron-deuteron breakup cross section for a three-body system at rest in the nuclear medium. Solid line represents isolated breakup cross section. Other lines are for different densities at the temperature $T=10$ MeV.

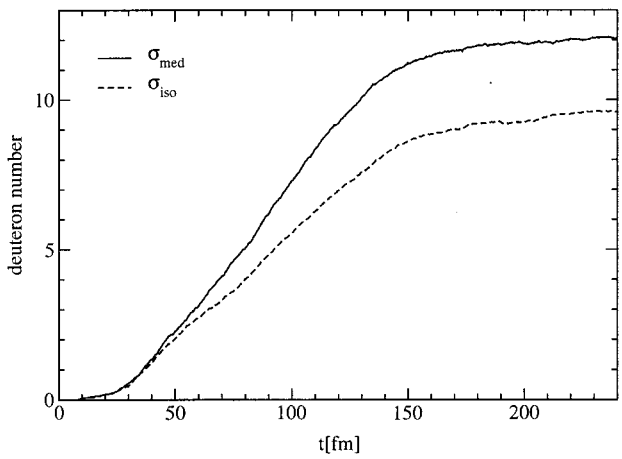

FIG. 3. Integrated deuteron number as a function of elapsed collision time when utilizing in-medium (upper curve) and isolated (lower curve) rates from BUU simulation with $F_{cut}=0.15$.

tion of the Mott momenta for a temperature of $T=10$ MeV and a wide density range. Note, that the cutoff values for both triton/helion and deuteron can be chosen to be approximately the same. We find only a slight variation of F_{cut} on the temperature ($F_{cut}\simeq 0.17$ for $T=5$ MeV). To illustrate sensitivity to different F_{cut}, we have plotted the Mott lines for $F_{cut}=0.10$ and $F_{cut}=0.20$ in Fig. 1. A *larger* value of F_{cut} makes the space for bound states *larger*. We shall study the influence of the Mott momentum on the results of reaction simulations. The direct implementation of the t matrix calculation for the Mott momenta into the BUU simulation requires the calculation of a local temperature that is very time consuming. Therefore we will use the geometrical model, with a properly adjusted global value of F_{cut}, to account for the Mott effect in the numerical solution of Eq. (1).

In Eq. (4) we give the relation between the isolated three-particle transition operators and the total deuteron break up cross section. The same equation is appropriate in defining the medium-dependent cross section now in terms of the medium-dependent transition operator U given in Eq. (18). The total deuteron break-up cross section can be used in the collision integrals (2) and (3), as, e.g., has been demonstrated in Ref. [1]. For illustration, we show in Fig. 2 the in-medium break-up cross section at a temperature of $T=10$ MeV for the three-body system at rest in the nuclear medium, which was explored to a larger extend in Refs. [9,11,14]. The solid line represents the isolated cross section that reproduces the experimental breakup data; other lines correspond to different nuclear matter densities. The influence of the in-medium cross sections on characteristic kinetic quantities such as the chemical relaxation time is significant as has been demonstrated in Ref. [14].

For a specific heavy ion reaction, we now investigate (i) to what extend the medium dependence of the deuteron breakup cross section affects the observables and, in particular, the deuteron production and (ii) how sensitive are the observables to the parametrization of the Mott momenta. To this end, we consider the central collision ^{129}Xe+^{119}Sn at $E/A=50$ MeV and compare our theoretical results with the experimental data of the INDRA Collaboration [21].

To provide a first impression on how the use of in-medium rates in the Boltzmann collision integrals influences the outcome of the reaction simulation, Fig. 3 shows the total deuteron number (gain minus loss) as a function of elapsed time. The upper line is for the in-medium cross sections depending on the local density and the temperature. The lower line is for the isolated cross sections that reproduce the experimental scattering data. Gain and loss rates are enhanced by use of in-medium rates such that the net effect leads to a significant increase in the total number of deuterons because equilibrium is maintained down to lower densities and temperatures. In both simulations, we have used $F_{cut}=0.15$. Though the increase in the deuteron number may be significant, the theoretical value of the total deuteron number may be still too uncertain for a direct comparison to data. This is because the effect of the heavier $A\geqslant 4$ clusters is not yet included in our simulation.

The influence of the different medium effects on the spectral distribution of proton, deuteron, triton, and helion clusters is shown in Fig. 4. Solid line shows the results of our calculation using the *medium-dependent* cross sections in the collision integrals of the BUU simulation. Dashed line shows the spectra obtained using the *isolated* cross sections that reproduce the experimental data. In all cases we have included the Mott effect and for the solid and the dashed lines we use $F_{cut}=0.15$. To demonstrate the sensitivity to different Mott momenta, the dotted line shows results obtained using $F_{cut}=0.20$ for medium-dependent rates. As explained in Refs. [9,11,14], the deuteron breakup cross section is strongly enhanced near the threshold. As a consequence, we find an enhancement of about 30% in the deuteron number in the energy range $E_{c.m.}\leqslant 50$ MeV if we compare the dashed line (for isolated deuteron breakup cross sections) to the solid line (for medium-dependent deuteron breakup cross sections). A larger absorption implies a larger production rate and maintaining the possible chemical equilibrium down to lower freeze-out densities. Inspecting the dotted line, we find, as expected, that the number of clusters increases with

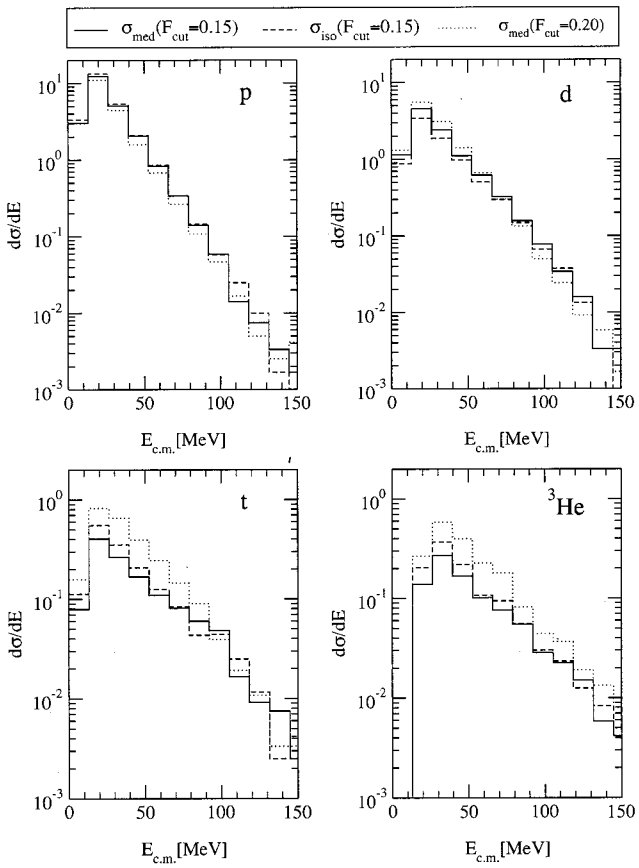

FIG. 4. Light charged particle spectra in the center of mass system for the reaction ^{129}Xe+^{119}Sn at 50 MeV/nucleon. Calculations with in-medium *Nd* reaction rates are represented by solid lines, while those with isolated *Nd* breakup cross sections are represented by dashed lines. In both cases $F_{\rm cut}=0.15$ is employed. Calculations with $F_{\rm cut}=0.20$ and in-medium reaction rates are represented by the dotted lines.

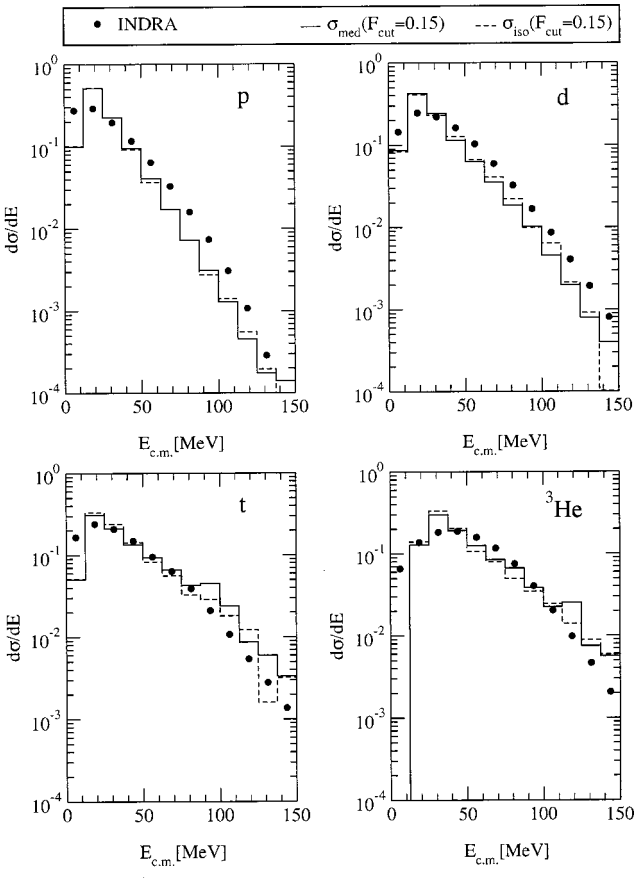

FIG. 5. Renormalized light charged light particle spectra in the center of mass system for the reaction ^{129}Xe+^{119}Sn at 50 MeV/nucleon. The filled circles represent the data of the INDRA Collaboration [21]. The solid line shows the calculations with the in-medium *Nd* reaction rates, while the dashed line shows a calculation using the isolated *Nd* breakup cross section; both with $F_{\rm cut}=0.15$.

the rise in $F_{\rm cut}$. Hence, relaxing the limitation of the allowed existence of a cluster (by using the same rates) leads to an enhanced production as the clusters become more stable. Also, simultaneously, the spectra appear steeper.

Figure 5 compares energy spectra of the light $A\leqslant 3$ clusters to INDRA data renormalized as in Ref. [21]. To compare to our calculations we renormalize our results in the same fashion as data, i.e., the areas below the respective curves are normalized to the same fixed value. As before the results obtained with the *medium-dependent* cross sections are represented by a solid line; the dashed line shows the results of the coupled BUU calculation using the *isolated* deuteron breakup cross sections. In both calculations we use $F_{\rm cut}=0.15$. Overall, the renormalization seems to reduce the effect of using different elementary rates in the collision integrals. For the deuteron, the *in-medium* rates lead to a marginally steeper shape. Differences at higher c.m. energies can be attributed to statistical fluctuations.

Considering now the three-nucleon clusters, we find the helion/triton energy spectrum in a reasonable agreement with the experimental data. The only in-medium effect that we

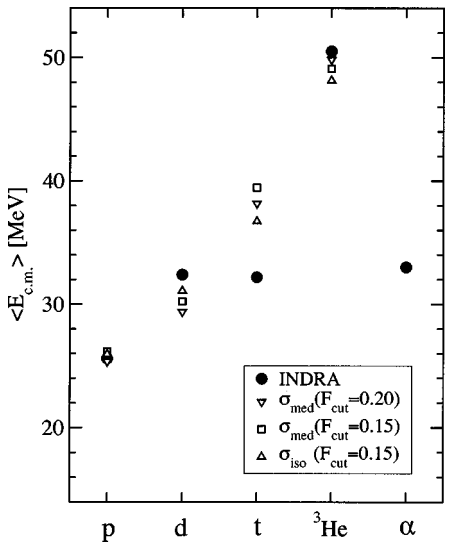

FIG. 6. Mean transverse energy of light charged fragments in the angular range of $-0.5\leqslant\cos\theta_{\rm c.m.}\leqslant 0.5$.

consider for the three-nucleon clusters is the Mott effect. A possible modification of the three-particle cluster formation and breakup rates is disregarded. The observed reduction, see Fig. 4, of the three-nucleon cluster production in the calculation using the medium deuteron breakup cross section is a response to the enhanced deuteron production. The apparent deviation from experiment in the lowest energy bin is likely related to a long-lived residue appearing in the simulation that in turn leads to an enhanced Coulomb barrier. This affects the lowest energies only and might be cured by allowing for fluctuations in the residue that would lead to the intermediate fragment production and, consequently, to the suppression of the Coulomb barrier. This is presently not accounted for in the model.

Finally, in Fig. 6 we show the measured values (filled circles) for the mean energies of the light clusters emitted in transverse direction along with the result of the calculation. As the experimental spectrum is not perfectly reproduced, see Fig. 5, this integrated observable also shows some discrepancy with the experimental data. The same remarks given for Fig. 5 hold for Fig. 6 as well. The changes due to different Mott momenta and use of in-medium rates are rather small in this observable. No theoretical results are given for α particles which are not yet included in the simulations.

V. CONCLUSION

Within the microscopic transport description of heavy-ion collision dynamics, we have demonstrated the influence of medium effects on some typical observables. The dominant medium effects are self-energy and statistical corrections, i.e., for clusters the Mott effect, and the change of reaction rates that lead to faster time scales. The magnitude of the in-medium effects depends on the density and the energy deposited in the system. The basis for microscopic calculations of the in-medium effects is the cluster mean-field expansion or Dyson equation approach. The effective few-body equations resulting from these approaches are numerically solved using well established and controllable few-body techniques. The chosen example of a heavy-ion reaction is ^{129}Xe+^{119}Sn at beam energy of 50 MeV/nucleon. Both effects, Mott and rate modification, affect the considered observables in a comparable fashion. Presently, we have implemented the modifications of rates for the three-body breakup and formation only. However, through the coupling of the Boltzmann equations, the number of three-nucleon clusters is also affected. We argue that a complete treatment requires a similar approach for the three- and four-nucleon clusters before a decisive comparison with experiments can be made. First calculations for the Mott effect of the α particle solving a proper four-body equation has been given in [15].

ACKNOWLEDGMENTS

This work has been supported by the Deutsche Forschungsgemeinschaft and by the National Science Foundation under Grant No. PHY-0070818. M.B. and C.K. thank the NSCL at MSU for the warm hospitality extended to them during their respective stays.

[1] P. Danielewicz and G.F. Bertsch, Nucl. Phys. **A533**, 712 (1991).
[2] P. Danielewicz and Q. Pan, Phys. Rev. C **46**, 2002 (1992).
[3] H. Stöcker and W. Greiner, Phys. Rep. **137**, 277 (1986).
[4] C. Fuchs and H.H. Wolter, Nucl. Phys. **A589**, 732 (1995).
[5] J. Aichelin, Phys. Rep. **202**, 233 (1991), and references therein.
[6] G. Peilert *et al.*, Phys. Rev. C **46**, 1457 (1992).
[7] *Multifragmentation*, edited by H. Feldmeier, J. Knoll, W. Nörenberg, and J. Wambach (GSI, Darmstadt, 1999).
[8] E.O. Alt, P. Grassberger, and W. Sandhas, Nucl. Phys. **B2**, 167 (1967).
[9] M. Beyer, G. Röpke, and A. Sedrakian, Phys. Lett. B **376**, 7 (1996).
[10] M. Beyer, Habilitation thesis, Rostock, 1997 (in German).
[11] M. Beyer and G. Röpke, Phys. Rev. C **56**, 2636 (1997).
[12] M. Beyer, Few-Body Syst., Suppl. **10**, 179 (1999).
[13] M. Beyer, W. Schadow, C. Kuhrts, and G. Röpke, Phys. Rev. C **60**, 034004 (1999).
[14] C. Kuhrts, M. Beyer, and G. Röpke, Nucl. Phys. **A668**, 137 (2000).
[15] M. Beyer, S. A. Sofianos, C. Kuhrts, G. Röpke, and P. Schuck, Phys. Lett. B **488**, 247 (2000).
[16] L.P. Kadanoff and G. Baym, *Quantum Theory of Many-Particle Systems* (McGraw-Hill, New York, 1962); A.L. Fetter and J.D. Walecka, *Quantum Theory of Many-Particle Systems* (McGraw-Hill, New York, 1971).
[17] G. Röpke, M. Schmidt, L. Münchow, and H. Schulz, Nucl. Phys. **A399**, 587 (1983).
[18] J. Dukelsky, G. Röpke, and P. Schuck, Nucl. Phys. **A628**, 17 (1998), and references therein.
[19] G. Röpke, L. Münchow, and H. Schulz, Nucl. Phys. **A379**, 536 (1982).
[20] G. Röpke, Phys. Lett. B **215**, 281 (1987).
[21] INDRA Collaboration, D. Gorio *et al.*, Eur. Phys. J. A **7**, 245 (2000), and references therein.
[22] W. Glöckle, *The Quantum Mechanical Few-Body Problem* (Springer, Berlin/New York, 1983); I. R. Afnan and A. W. Thomas, in *Modern Three Hadron Physics*, edited by A. W. Thomas (Springer, Berlin, 1977), p. 1; E. W. Schmidt and H. Ziegelmann, *The Quantum Mechanical Three-Body Problem* (Pergamon, Oxford, 1974); W. Sandhas, Acta Phys. Austriaca, Suppl. **IX**, 57 (1972); V. B. Belyaev, *Lectures on the Theory of Few-Body Systems* (Spinger, Berlin, 1990).
[23] J. Eichler, T. Marumori, and K. Takada, Prog. Theor. Phys. **40**, 60 (1968).
[24] P. Schuck, F. Villars, and P. Ring, Nucl. Phys. **A208**, 302 (1973).
[25] D. Zubarev, V. Morozov, and G. Röpke, *Statistical Mechanics of Nonequlibrium Processes I,II* (Akademie, Verlag, Berlin, 1997).
[26] Y. Yamaguchi, Phys. Rev. **95**, 1628 (1954).
[27] A. Schnell, Ph.D. thesis, Rostock, 1996; (private communication).